

Supporting Information

Capture of $[\text{Bi}_4]^{6-}$ and $[\text{Bi}_3]^{5-}$ Anions by $[\text{Rh}(\text{L})]^+$ (L=COD) Cations in the *closo* Heteroatomic Clusters $\{\text{Bi}_4[\text{Rh}(\text{L})_4]^{2-}$ and $\{\text{Bi}_3[\text{Rh}(\text{L})_3]^{2-}$

Zhibing Liang, lifang Lin, Yuanwei Liang*, Yi Wang*

E-mail: liangyw@gdou.edu.cn; ywangcm@gmail.com

1. Experimental Procedures

All reactions were performed under an inert atmosphere of dry nitrogen or argon in a dry box (Vacuum Atmospheres Co) or using standard Schlenk techniques. Melts of a Zintl phase of nominal composition K_5Bi_4 were prepared by fusion ($\sim 1100^\circ\text{C}$) of stoichiometric ratios of the corresponding elements. **Caution: Synthesis of Zintl phases is highly exothermic. Full personal protective equipment and blast shields should be used at all times!** Ethylenediamine was purified via long-path distillation over sodium metal. Other solvents were purified by distillation from sodium benzophenone ketyl radical under a dinitrogen atmosphere. $\text{Rh}(\text{COD})(\text{Acac})(\text{COD}= 1,5\text{-cyclooctadiene, Acac}= \text{acetylacetonate})$ and $\text{Rh}(\text{COD})(\text{Cp})(\text{Cp}= \text{cyclopentadienyl})$ were synthesized according to the literature.^[1] 1,4,7,10,13,16-Hexaoxacyclooctadecane (18-crown-6 ether, >98%, TCI America) and 4,7,13,16,21,24-Hexaoxa-1,10-diazabicyclo[8.8.8]hexacosane(2,2,2-crypt, >98%, Acros Organic) were used as received. Negative ion mode electrospray ionization mass spectrometry (ESI-MS) experiments were carried out on the CH_3CN solution of the according crystal samples through a JEOL AccuTOF-CS MS spectrometer with source temperature of 100°C , desolvation temperature of 200°C , capillary voltage of 2.1 kV and cone voltage of 65V. The samples were prepared in an N_2 -filled glovebox and introduced into the spectrometer through a 2.5 ml air-tight syringe. Energy dispersive X-ray spectroscopy (EDX) analysis was performed on Hitachi SU-70 SEM, operated at an acceleration voltage of 25 keV (**Note:** EDX is only a semiquantitative analysis method, which usually can't give the accurate ratio of elements. Deviations are rather common in the EDX characterization of Zintl clusters which can be ascribed to the irregular surfaces of the crystals after exposure to air.). Data acquisition was performed with an accumulation time of 180s. All the NMR experiment was performed on a Bruker AV-400 MHz spectrometer at room temperature. ^1H NMR and ^{13}C NMR spectra were calibrated to residual ^1H and ^{13}C chemical shifts of acetonitrile- d_3 , respectively.

Synthesis of $[\text{K}(18\text{-crown-6})]_2\{\text{Bi}_4[\text{Rh}(\text{COD})]_4\} \cdot 2\text{en} \cdot 2\text{tol}$ 182.0mg (1.76mmol) of " K_5Bi_4 " and 228.5 mg (8.65mmol) of 18-Crown-6 were weighed out into a 10 mL scintillation vial. Then *ca.* 7mL of ethylenediamine was added. The reaction mixture was stirred for 30 min, resulting in a blue-green solution, into which $\text{Rh}(\text{COD})(\text{acac})$ (46.3mg, 1.49mmol) was added as solids. The reaction mixture was

stirred at room temperature for 2h. The resulting dark brown red solution were filtered through glass wool and transferred into a test tube (12×75mm) and then carefully layered with **6ml** toluene. After about ten days, large black block-like crystals of $[K(18\text{-crown-6})]_2[Bi_4[Rh(COD)]_4] \cdot 2en \cdot 2tol$ were high reproducibly obtained in approximately 16% yield based on the precursor $Rh(COD)(acac)$ used.

Synthesis of $[K(2,2,2\text{-crypt})]_2[Bi_3[Rh(COD)]_3] \cdot 0.5en$ In a vial, precursor with the nominal composition K_5Bi_4 (103.1mg, 0.1mmol) and 2,2,2-crypt (112.2 mg, 0.3mmol) were added into 2ml ethylenediamine (en), a blue-green solution was resulted after stirring at room temperature for 30 min. $Rh(COD)(Cp)$ (20.7mg, 0.075mmol) was then added into the vial above as solid. The solution mixtures were then stirred at room temperature for 2h, resulting in a brown-red solution, the reaction mixture was then filtered through tightly packed glass wool. The filtrate was layered with another 3ml toluene. After about a week, small black needle-like crystals of $[K(2,2,2\text{-crypt})]_2[Bi_3[Rh(COD)]_3] \cdot 0.5en$ were observed in the bottle of the tube, with a yield of 23% based on the transition metal complex $Rh(COD)(Cp)$ used.

X-ray crystal-structure determination (1). $[K(18\text{-crown-6})]_2[Bi_4[Rh(COD)]_4] \cdot 2en \cdot 2tol$ (GDOU01) A suitable single crystal was selected and measured on a Bruker Smart Apex II CCD diffractometer [2]. The crystal was kept at 150(2) K during data collection. The integral intensity were correct for absorption using SADABS software [3] using multi-scan method. Resulting minimum and maximum transmission are 0.108 and 0.196 respectively. The structure was solved with the ShelXT-2014 (Sheldrick, 2015a) [4] program and refined with the ShelXL-2015 (Sheldrick, 2015c) [5] program and least-square minimisation using ShelX software package [6]. Number of restraints used = 1130. 1 of 2 $[K(18\text{-crown-6})]^+$ ions and en solvent molecules binding K-crown ions are disordered in 2 alternative orientations and therefore were refined with geometry restrained to be similar and atomic displacement parameters to correspond to rigid body motions and to be similar as well. H atoms were positioned from geometric considerations and refined as riding on the attached atoms with Uiso constrained to be 20% (50% for methyl group) larger than Ueqv of the attached atom. Orientation of methyl groups was optimized.

(2). **$[K(2,2,2\text{-crypt})]_2[Bi_3[Rh(COD)]_3] \cdot 0.5en$** A suitable single crystals of $C_{61}H_{112}Bi_3K_2N_5O_{12}Rh_3$ (GDOU02) was selected and measured on a Pulatus 1M diffractometer [2]. The crystal was kept at 150(2) K during data collection. The integral intensity was correct for absorption using SADABS software [3] using multi-scan method. Resulting minimum and maximum transmission are 0.3586 and 0.4235 respectively. The structure was solved with the ShelXT (Sheldrick, 2015a) [4] program and refined with the ShelXL (Sheldrick, 2015c) [5] program and least-square minimisation using ShelX software package [6]. Number of restraints used = 13.

References:

1. J. Chatt and L. M. Venanzi, *J. Chem. Soc.*, 1957, **744**, 4735– 4741.
2. Bruker (2010). Apex2. Bruker AXS Inc., Madison, Wisconsin, USA.
3. Krause, L., Herbst-Irmer, R., Sheldrick, G.M., Stalke, D. (2015). *J. Appl. Cryst.* 48, 3-10.
4. Sheldrick, G. M. (2015a). *Acta Cryst.* A17, 3-8.
5. Sheldrick, G. M. (2015c). *Acta Cryst.* C17, 3-8.
6. Dolomanov, O.V., Bourhis, L.J., Gildea, R.J, Howard, J.A.K. & Puschmann, H. (2009), *J. Appl. Cryst.* 42, 339-341.

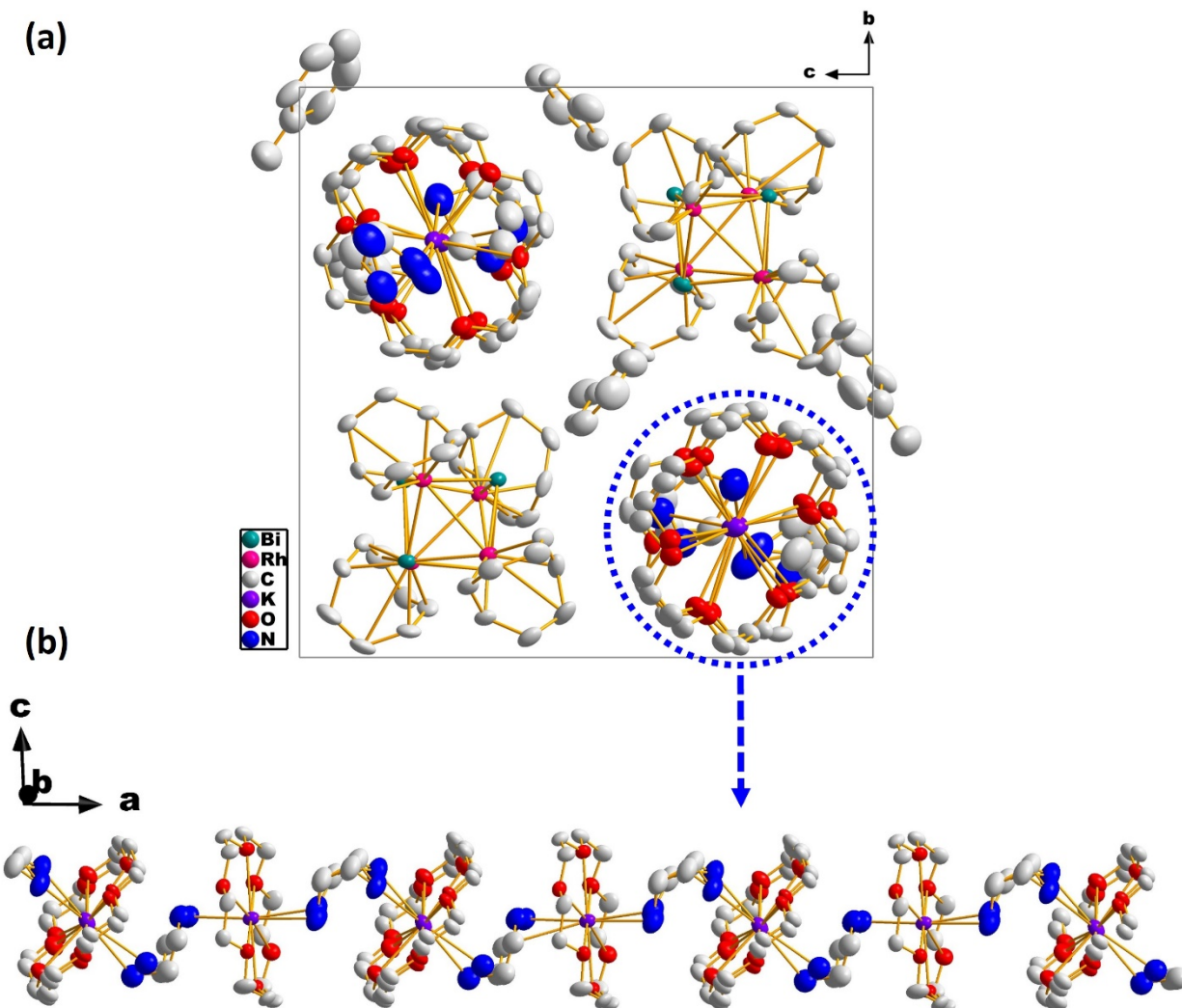


Figure S1 Crystal structure of the salt $[K(18\text{-crown-}6)]_2[Bi_4[Rh(COD)]_4] \cdot 2en \cdot 2tol$: (a) the unit cell structure, (b) the ${}^{\infty}_1[-en - [K(18crown6)] - en -]_+$ one dimension chain, with thermal ellipsoids drawn at 50% probability and hydrogen atoms omitted for clarity.

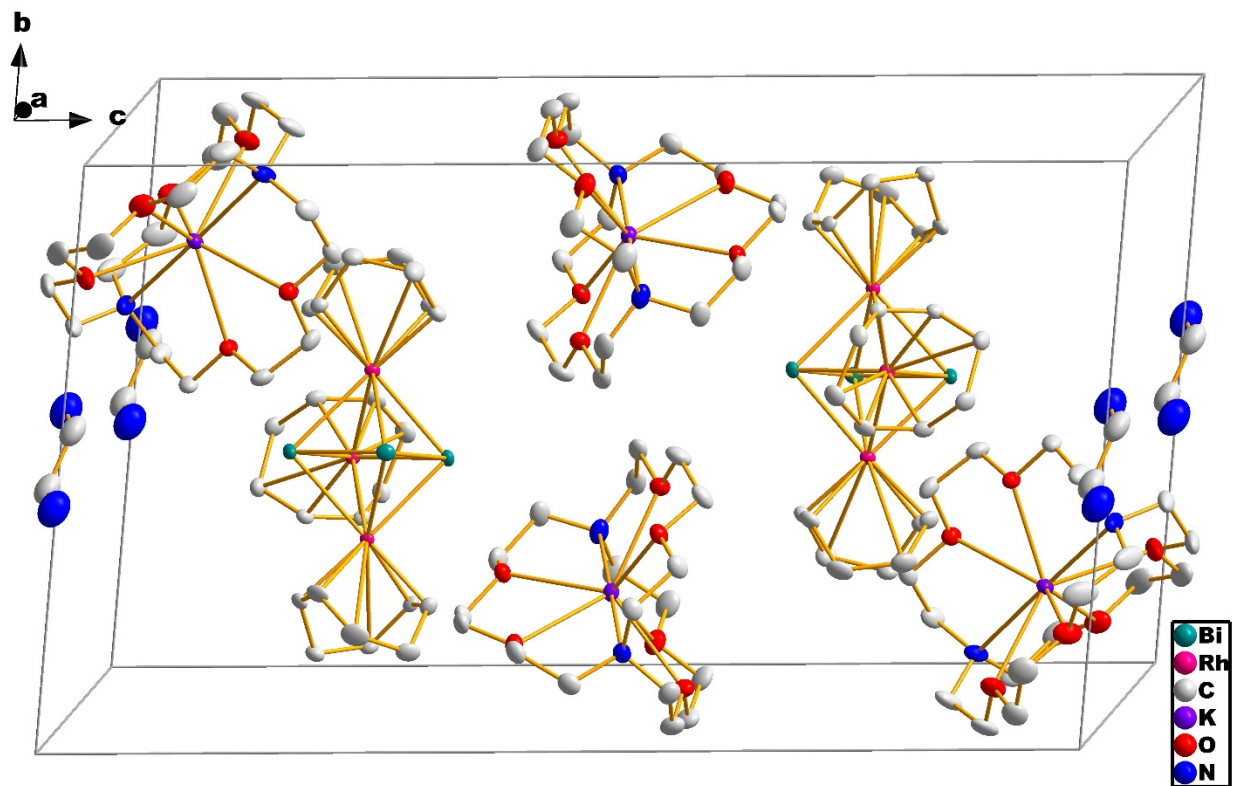


Figure S2. The unit cell structure of the salt of $[K(2,2,2\text{-crypt})]_2[Bi_3[Rh(COD)]_3] \cdot 0.5en$ with thermal ellipsoids drawn at 50% probability and hydrogen atoms omitted for clarity.

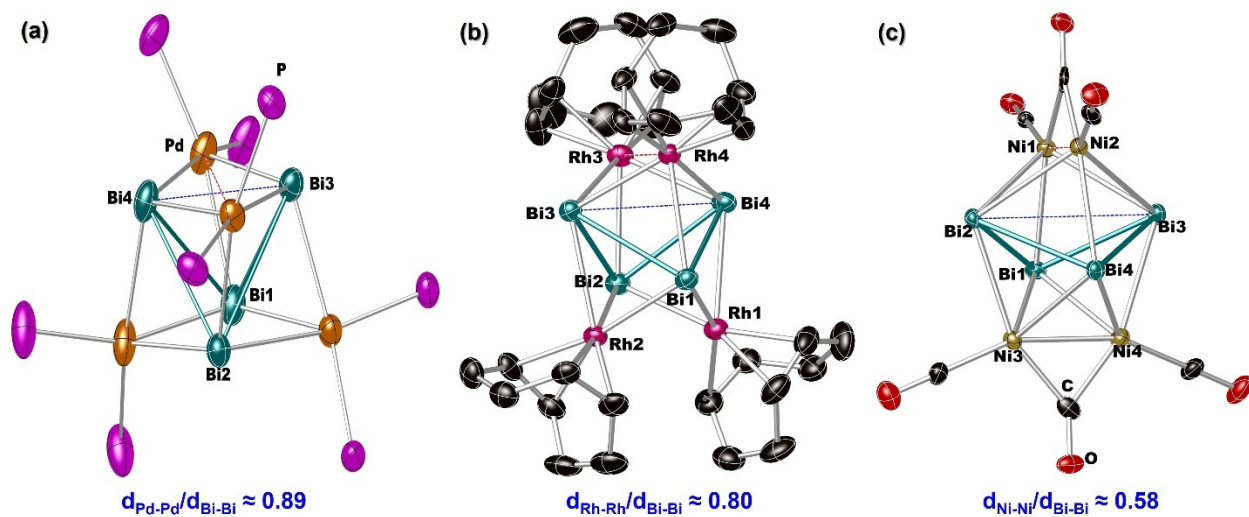


Figure S3 Crystal structure of cluster anions (a) $[\text{Bi}_4\text{Pd}_4(\text{PPh}_2\text{Me})_8]^{2+}$ where the PPh_2Me ligand was denoted by the P atom, (b) $\{\text{Bi}_4[\text{Rh}(\text{COD})]_4\}^{2-}$ and (c) $[\text{Bi}_4\text{Ni}_4(\text{CO})_6]^{2-}$ with thermal ellipsoid set at 50% probability level.

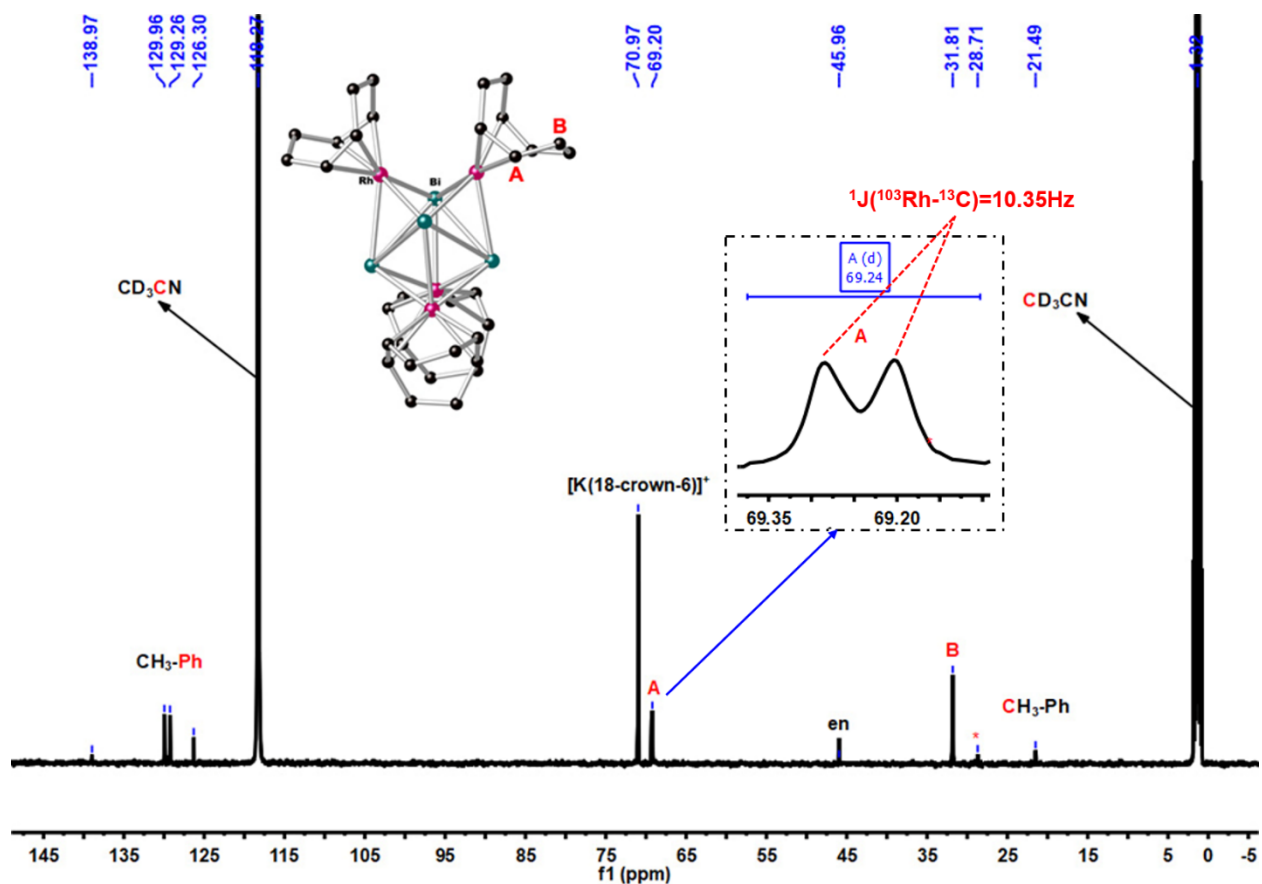


Figure S4 ^{13}C NMR of the crystal of the anion $\{\text{Bi}_4[\text{Rh}(\text{COD})]_4\}^{2-}$ in CD_3CN , in which the Rh-C couplings with $^1J(^{103}\text{Rh-}^{13}\text{C}) = 10.35\text{ Hz}$ were observed.

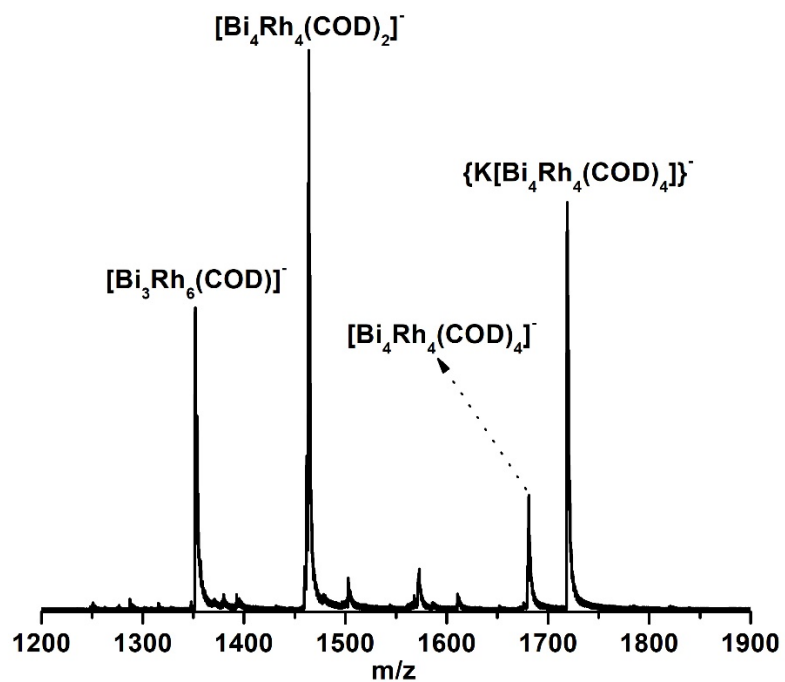


Figure S5 ESI-MS of the crystal sample of the cluster anion $\{Bi_4[Rh(COD)]_4\}^{2-}$ in CH_3CN in negative ion mode.

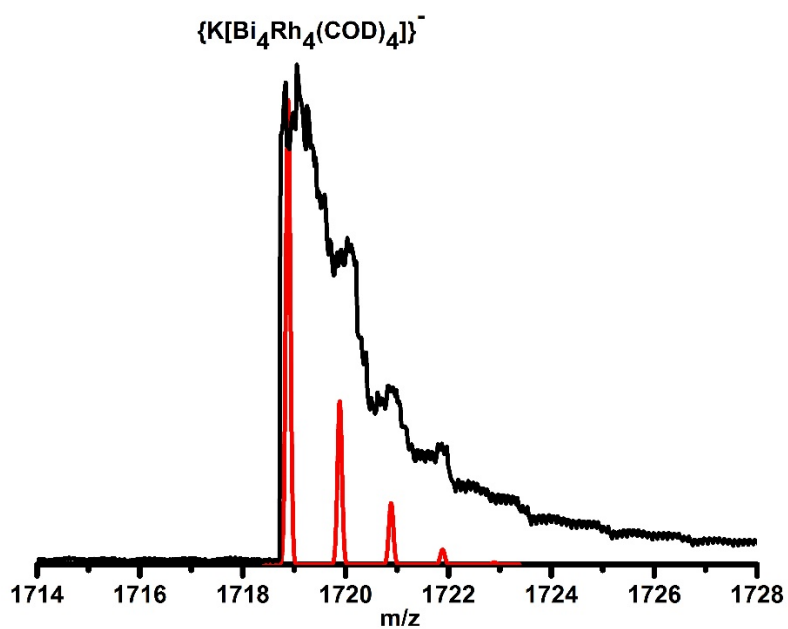


Figure S6 Measured (black) and simulated (red) spectra of the $\{K[Bi_4[Rh(COD)]_4]\}^-$ anion.

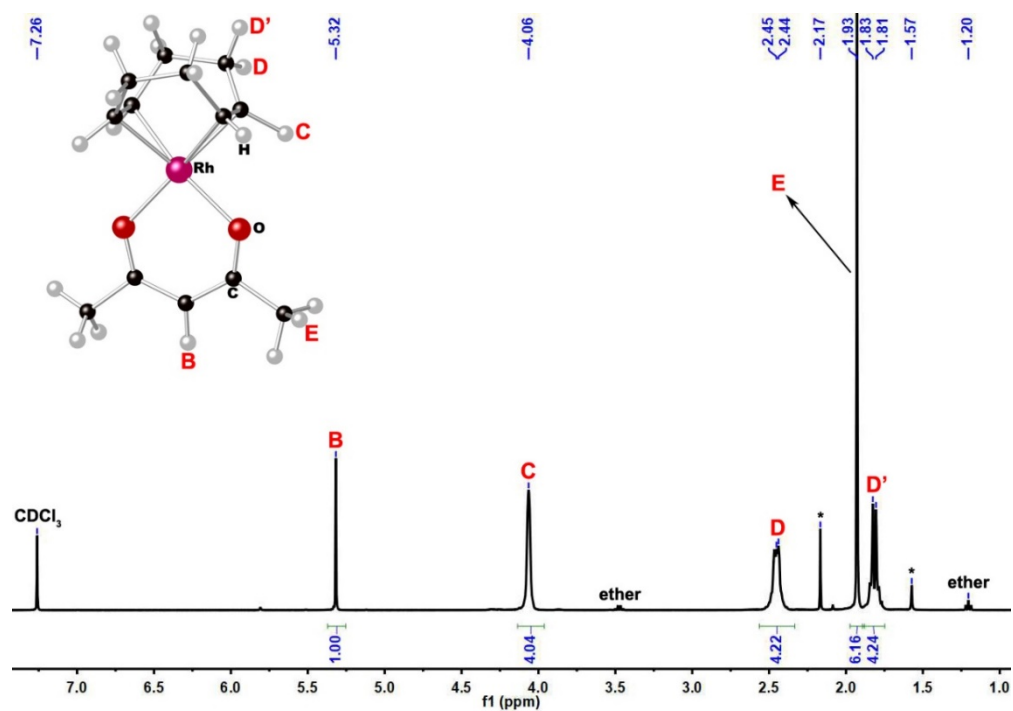


Figure S7 ^1H NMR of $\text{Rh}(\text{COD})(\text{Acac})$ in CDCl_3 at room temperature, with all H atoms being labeled.

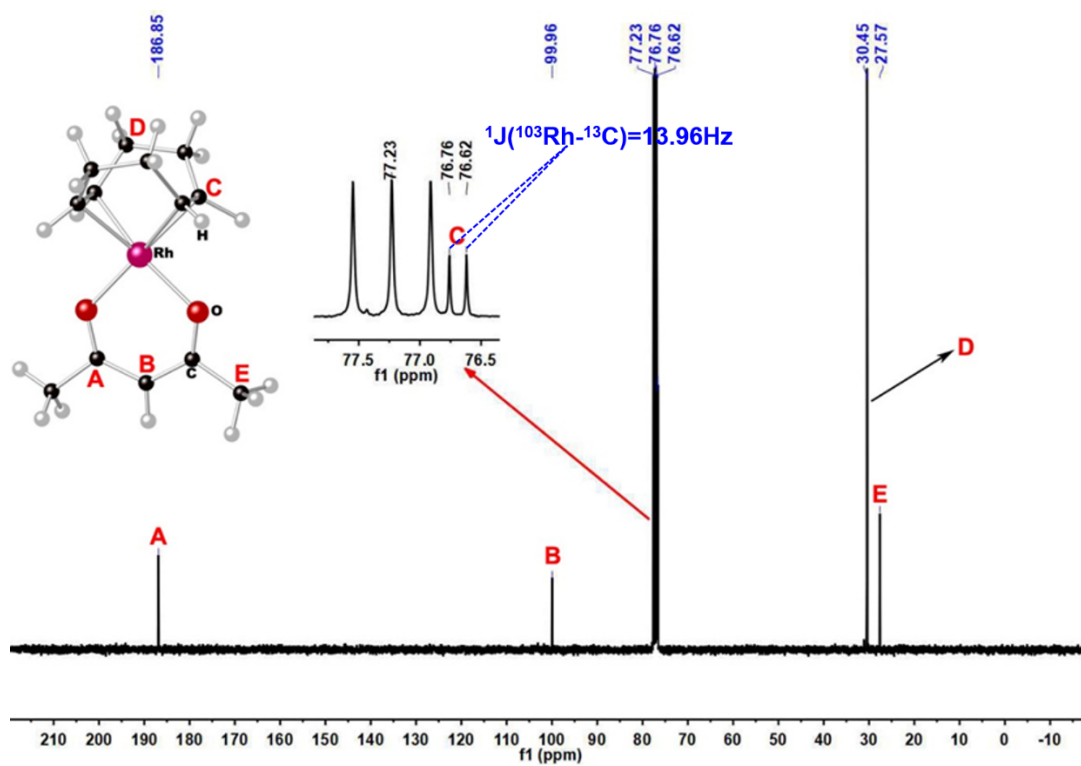


Figure S8 ^{13}C NMR of $\text{Rh}(\text{COD})(\text{Acac})$ in CDCl_3 at room temperature, with all C atoms being labeled and the Rh-C couplings $^1J(^{103}\text{Rh}-^{13}\text{C})=13.96\text{Hz}$.

Table S1 Selected bond distances and bond angles of the cluster anion $\{\text{Bi}_4[\text{Rh}(\text{COD})]_4\}^{2-}$ (1).

Bond distances (Å)							
Bi1-Rh2	2.7012(8)	Bi- Rh1	2.7420(8)	Bi1-Rh4	2.9117(8)	Bi2-Rh1	2.7170(8)
Bi2-Rh2	2.7362(8)	Bi2-Rh3	2.9552(8)	Bi3-Rh4	2.7196(8)	Bi3-Rh3	2.7292(7)
Bi3-Rh2	2.9373(7)	Bi4-Rh3	2.7082(8)	Bi4-Rh4	2.7419(7)	Bi4-Rh1	2.9116(8)
Bi1-Bi4	3.1663(5)	Bi1-Bi3	3.2693(4)	Bi2-Bi3	3.1620(4)	Bi2-Bi4	3.2289(5)
Rh1-Rh2	3.0798(10)	Rh3-Rh4	3.0607(10)				
Rh1-C14	2.155(9)	Rh1-C18	2.158(10)	Rh1-C11	2.181(9)	Rh1-C15	2.183(10)
Rh2-C25	2.154(9)	Rh2-C21	2.167(9)	Rh2-C28	2.170(10)	Rh2-C24	2.182(8)
Rh3-C38	2.170(10)	Rh3-C34	2.179(9)	Rh3-C35	2.183(9)	Rh3-C31	2.190(10)
Rh4-C44	2.136(10)	Rh4-C48	2.158(9)	Rh4-C45	2.176(11)	Rh4-C41	2.190(9)
C11-C18	1.413(14)	C14-C15	1.403(15)	C31-C38	1.386(16)	C34-C35	1.420(15)
C41-C48	1.407(13)	C44-C45	1.372(15)	C21-C28	1.394(13)	C24-C25	1.403(13)
Bond angles (°)							
Rh2-Bi-Rh1	68.91(2)	Rh2-Bi1-Rh4	109.18(2)	Rh1-Bi1-Rh4	110.47(2)	Rh2-Bi1-Bi4	99.590(19)
Rh1-Bi1-Bi4	58.523(18)	Rh4-Bi1-Bi4	53.432(15)	Rh2-Bi1-Bi3	58.008(16)	Rh1-Bi1-Bi3	97.357(18)
Rh4-Bi1-Bi3	51.814(16)	Bi4-Bi1-Bi3	73.056(11)	Rh1-Bi2-Rh2	68.77(2)	Rh1-Bi2-Rh3	108.89(2)
Rh2-Bi2-Rh3	110.29(2)	Rh1-Bi2-Bi3	100.471(18)	Rh2-Bi2-Bi3	59.211(16)	Rh3-Bi2-Bi3	52.863(15)
Rh1-Bi2-Bi4	57.875(18)	Rh2-Bi2-Bi4	97.346(18)	Rh3-Bi2-Bi4	51.712(17)	Bi3-Bi2-Bi4	73.664(11)
Rh4-Bi3-Rh3	68.35(2)	Rh4-Bi3-Rh2	107.92(2)	Rh3-Bi3-Rh2	111.02(2)	Rh4-Bi3-Bi2	99.507(18)
Rh3-Bi3-Bi2	59.678(17)	Rh2-Bi3-Bi2	53.155(16)	Rh4-Bi3-Bi1	57.300(17)	Rh3-Bi3-Bi1	97.169(18)
Rh2-Bi3-Bi1	51.257(15)	Bi2-Bi3-Bi1	72.975(11)	Rh3-Bi4-Rh4	68.33(2)	Rh3-Bi4-Rh1	110.42(2)
Rh4-Bi4-Rh1	110.47(2)	Rh3-Bi4-Bi1	100.089(18)	Rh4-Bi4-Bi1	58.525(17)	Rh1-Bi4-Bi1	53.434(15)
Rh3-Bi4-Bi2	58.927(18)	Rh4-Bi4-Bi2	97.435(19)	Rh1-Bi4-Bi2	52.212(17)	Bi1-Bi4-Bi2	73.468(11)

Table S2 Selected bond distances and bond angles of the cluster anion $\{\text{Bi}_3[\text{Rh}(\text{COD})]_3\}^{2-}$ (2).

Bond distances (Å)							
Bi1-Rh1	2.7549(2)	Bi1-Rh2	2.7559(2)	Bi1-Rh3	2.7641(2)	Bi2-Rh3	2.8885(3)
Bi2-Rh1	2.9079(2)	Bi3-Rh2	2.7276(2)	Bi3-Rh3	2.7437(2)	Bi3-Rh1	2.7598(2)
Bi1-Bi2	2.96867(19)	Bi2-Bi3	2.9592(2)	Rh1-Rh2	2.9316(3)	Rh2-Rh3	2.9383(3)
Rh1-C15	2.131(3)	Rh1-C11	2.145(3)	Rh1-C12	2.163(3)	Rh1-C16	2.168(3)
Rh2-C22	2.138(3)	Rh2-C26	2.144(3)	Rh2-C21	2.146(3)	Rh2-C25	2.152(3)
Rh3-C32	2.139(3)	Rh3-C36	2.142(3)	Rh3-C31	2.152(3)	Rh3-C35	2.168(3)
C11-C12	1.410(4)	C15-C16	1.416(4)	C21-C22	1.409(4)	C25-C26	1.415(4)
C31-C32	1.415(4)	C35-C36	1.422(4)				
Bond angles (°)							
Rh1-Bi1-Rh2	64.278(7)	Rh1-Bi1-Rh3	92.450(7)	Rh2-Bi1-Rh3	64.322(7)	Rh1-Bi1-Bi2	60.933(5)
Rh2-Bi1-Bi2	96.089(7)	Rh3-Bi1-Bi2	60.387(6)	Rh3-Bi2-Rh1	86.866(7)	Rh3-Bi2-Bi3	55.947(6)
Rh1-Bi2-Bi3	56.111(5)	Rh3-Bi2-Bi1	56.297(6)	Rh1-Bi2-Bi1	55.902(5)	Bi3-Bi2-Bi1	79.513(6)
Rh2-Bi3-Rh3	64.964(7)	Rh2-Bi3-Rh1	64.582(7)	Rh3-Bi3-Rh1	92.788(8)	Rh2-Bi3-Bi2	96.925(7)
Rh3-Bi3-Bi2	60.723(6)	Rh1-Bi3-Bi2	61.004(5)	Bi1-Rh1-Bi3	86.855(7)	Bi1-Rh1-Bi2	63.166(6)
Bi3-Rh1-Bi2	62.885(6)	Bi1-Rh1-Rh2	57.876(6)	Bi3-Rh1-Rh2	57.178(6)	Bi2-Rh1-Rh2	93.677(8)
Bi3-Rh2-Bi1	87.473(7)	Bi3-Rh2-Rh1	58.241(6)	Bi1-Rh2-Rh1	57.846(6)	Bi3-Rh2-Rh3	57.782(6)
Bi1-Rh2-Rh3	57.974(6)	Rh1-Rh2-Rh3	85.516(8)	Bi3-Rh3-Bi1	86.992(7)	Bi3-Rh3-Bi2	63.331(6)
Bi1-Rh3-Bi2	63.317(6)	Bi3-Rh3-Rh2	57.255(6)	Bi1-Rh3-Rh2	57.703(6)	Bi2-Rh3-Rh2	93.940(8)

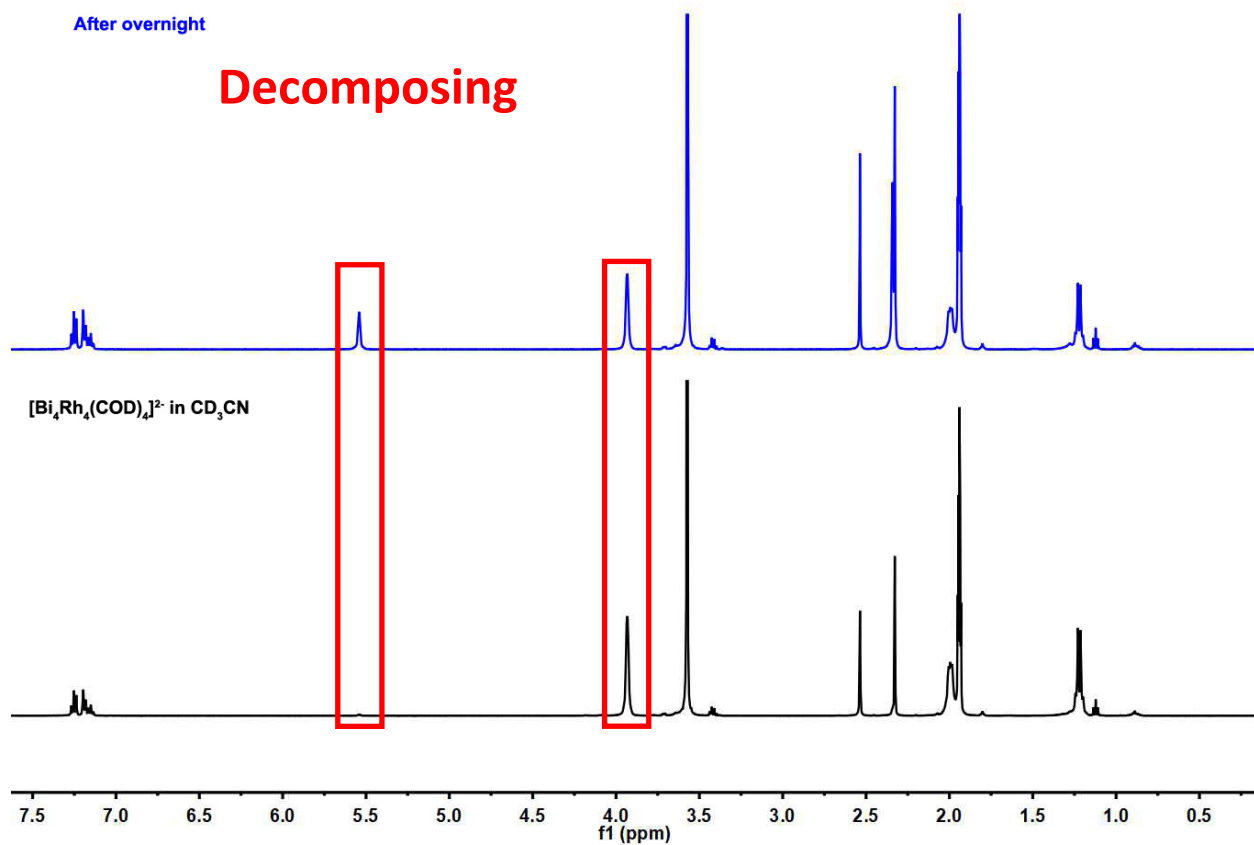


Figure S9 ^1H NMR of the crystal of the anion $\{\text{Bi}_4[\text{Rh}(\text{COD})]_4\}^{2-}$ in CD_3CN after overnight.

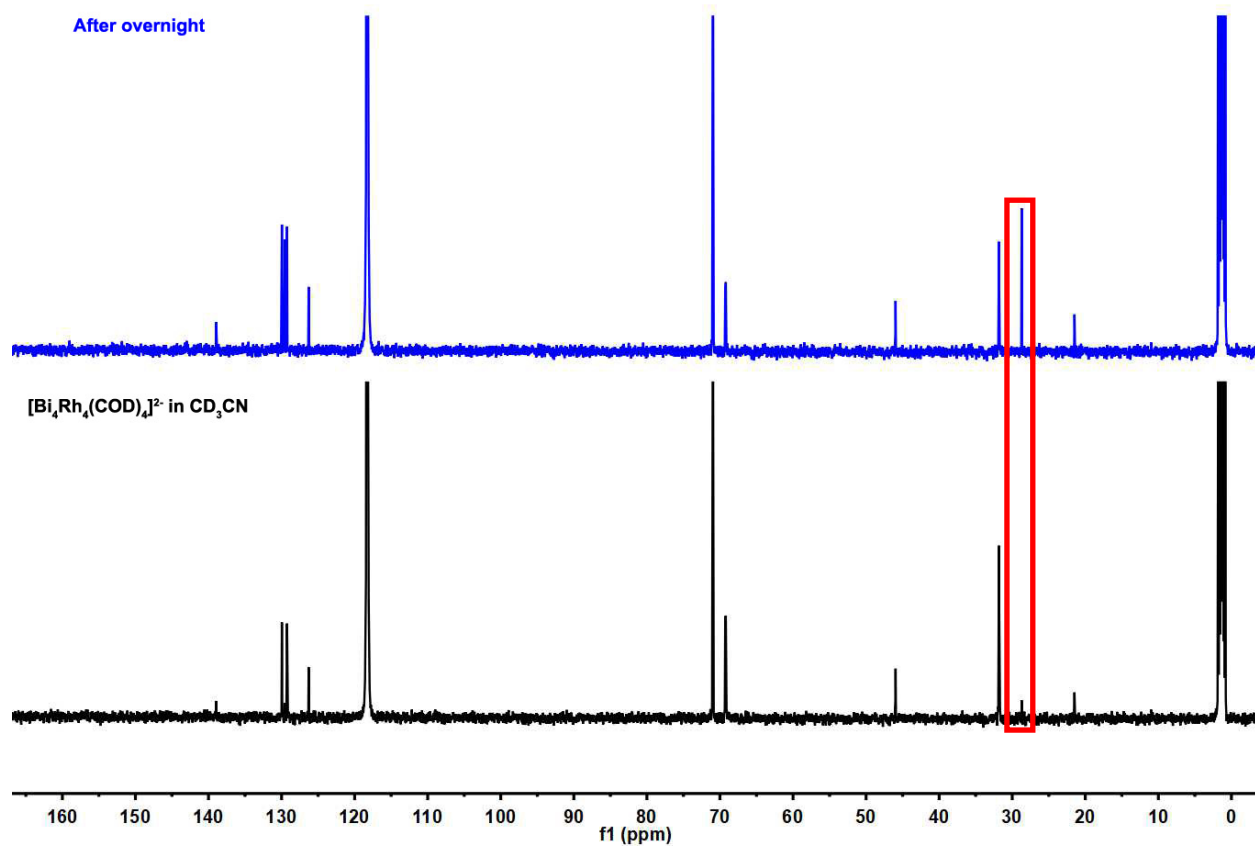


Figure S10 ^{13}C NMR of the crystal of the anion $\{\text{Bi}_4[\text{Rh}(\text{COD})_4]_4\}^{2-}$ in CD_3CN after overnight.

Table S3 Elemental analysis of the $[\text{K}(\text{18-crown-6})]_2\{\text{Bi}_4[\text{Rh}(\text{COD})_4]\} \cdot 2\text{en} \cdot 2\text{tol}$ crystals by EDX.

Element	AN	series	Net	[wt.%]	[norm. wt.%]	[norm. at.%]	Error in %
Carbon	6	K-series	42636	20.46665	18.52051	39.31018	2.269903
Oxygen	8	K-series	22062	35.13757	31.79641	50.66471	4.011884
Potassium	19	K-series	28606	3.819383	3.456205	2.253579	0.1404
Rhodium	45	L-series	111917	18.73877	16.95694	4.200877	0.634115
Bismuth	83	L-series	16008	32.34562	29.26994	3.570652	1.004609
			Sum:	110.508	100	100	
				<i>theoretical: K/Rh/Bi=1/2/2</i>	<i>expt.: K/Rh/Bi=1/1.9/1.6</i>		

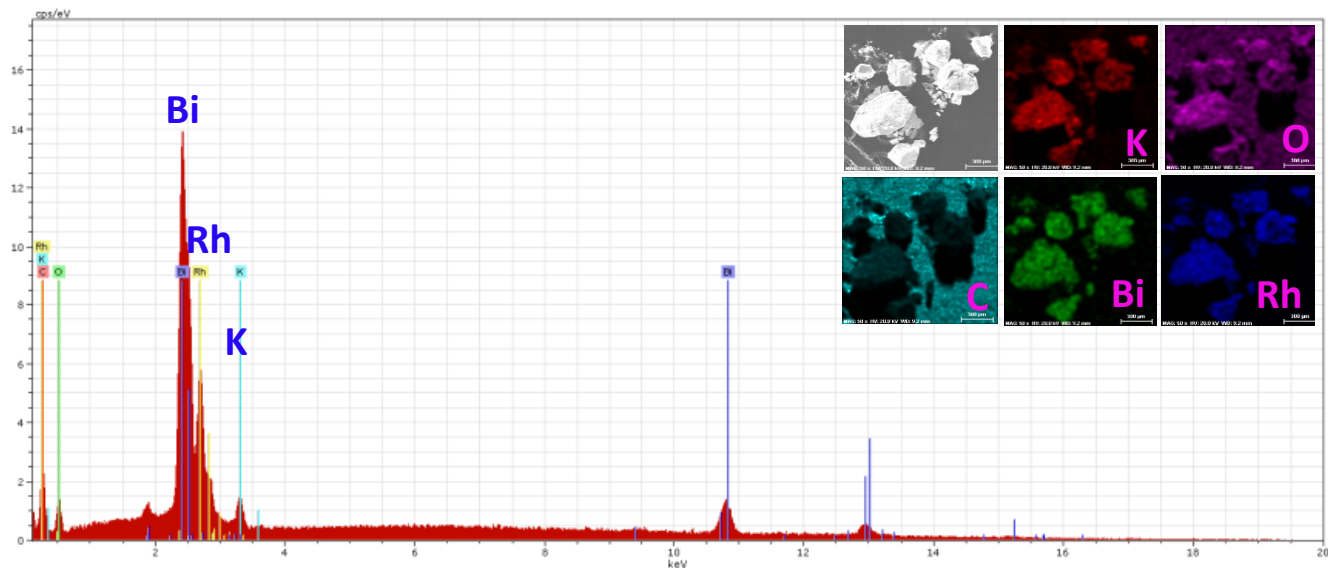


Figure S11 SEM image and EDX analysis of the $[K(18\text{-crown-}6)]_2[Bi_4[Rh(\text{COD})]_4] \cdot 2\text{en} \cdot 2\text{tol}$ crystals. No other elements heavier K, Bi and Rh were noticed.

Table S4 Elemental analysis of the $[K(2,2,2\text{-crypt})]_2[Bi_3[Rh(\text{COD})]_3] \cdot 0.5\text{en}$ crystals by EDX.

Element	AN	series	Net	[wt.%]	[norm. wt.%]	[norm. at.%]	Error in %
Carbon	6	K-series	304339	36.69238	38.06458	65.16279	3.827262
Oxygen	8	K-series	31162	19.67499	20.41078	26.23093	2.215409
Potassium	19	K-series	211598	7.481486	7.761274	4.081623	0.251049
Rhodium	45	L-series	250828	11.43076	11.85824	2.369406	0.396564
Bismuth	83	M-series	454124	21.11546	21.90512	2.155251	0.762714
			Sum:	96.39508	100	100	
<i>theoretical: K/Rh/Bi=2/3/3</i>				<i>expt.: K/Rh/Bi=1.9/1.1/1</i>			

Table S5. Rh-Rh bond lengths in heteroatomic polybismuth anions $[Bi_xRh_yL_z]^{q-}$ (Å)

$[Bi_xRh_yL_z]^{q-}$	$\{Bi_4[Rh(\text{COD})]_4\}^{2-}$ (1)	$\{Bi_3[Rh(\text{COD})]_3\}^{2-}$ (2)	$[Bi_7Rh_3(\text{CO})_3]^{2-}$ Ref.7	$[Bi@Rh_{12}(\text{CO})_{27}]^{3-}$ Ref.8	$[(Bi@Rh_{12}(\text{CO})_{26})_2Bi]^{5-}$ Ref.8	$[Bi@Rh_{14}(\text{CO})_{27}Bi_2]^{3-}$ Ref.8	
						A-type	B-type
Rh-Rh	3.0607(10)Å -3.0798(10)	2.9316(3)- 2.9383(3)	2.9925(16)- 3.0318(16)	2.8119(6)- 3.0792(6)	2.8050(17)-3.188(3)	2.754(4)- 3.117(4)	2.761(4)- 3.170(5)
Rh-Rh (av.)	3.0702	2.9349	3.009(1)	2.9832	2.9703	2.968	2.962

References:

7. Z. Li, D. Ouyang and L. Xu, *Chem. Commun.*, 2019, **55**, 6783-6786.

8. C. Femoni, G. Bussoli, I. Ciabatti, M. Ermini, M. Hayatifar, M. C. Iapalucci, S. Ruggieri and S. Zacchini, *Inorg. Chem.*, 2017, **56**, 6343-6351.

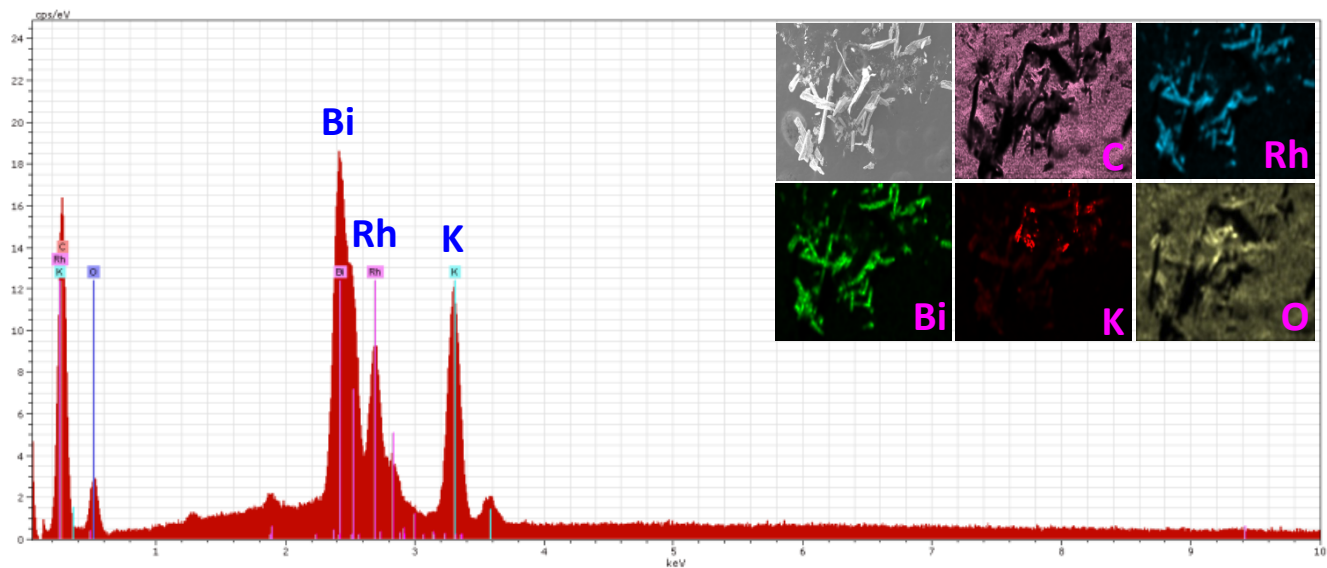


Figure S12 SEM image and EDX analysis of the $[K(2,2,2\text{-crypt})]_2[Bi_3[Rh(COD)]_3] \cdot 0.5en$ crystals. No other elements heavier K, Bi and Rh were noticed.

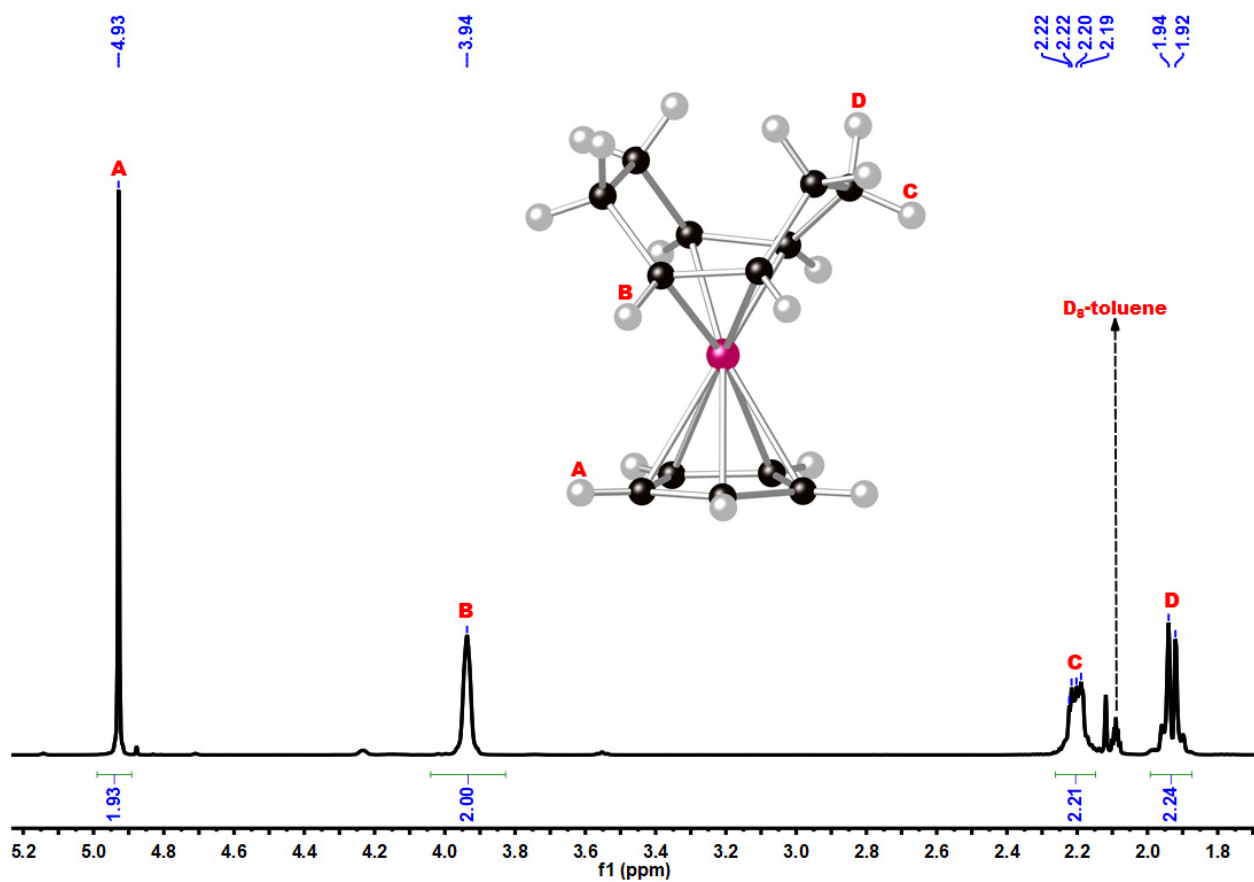


Figure S13 ^{13}C NMR of $CpRh(COD)$ in D_8 -toluene at room temperature, with all H atoms being labeled.

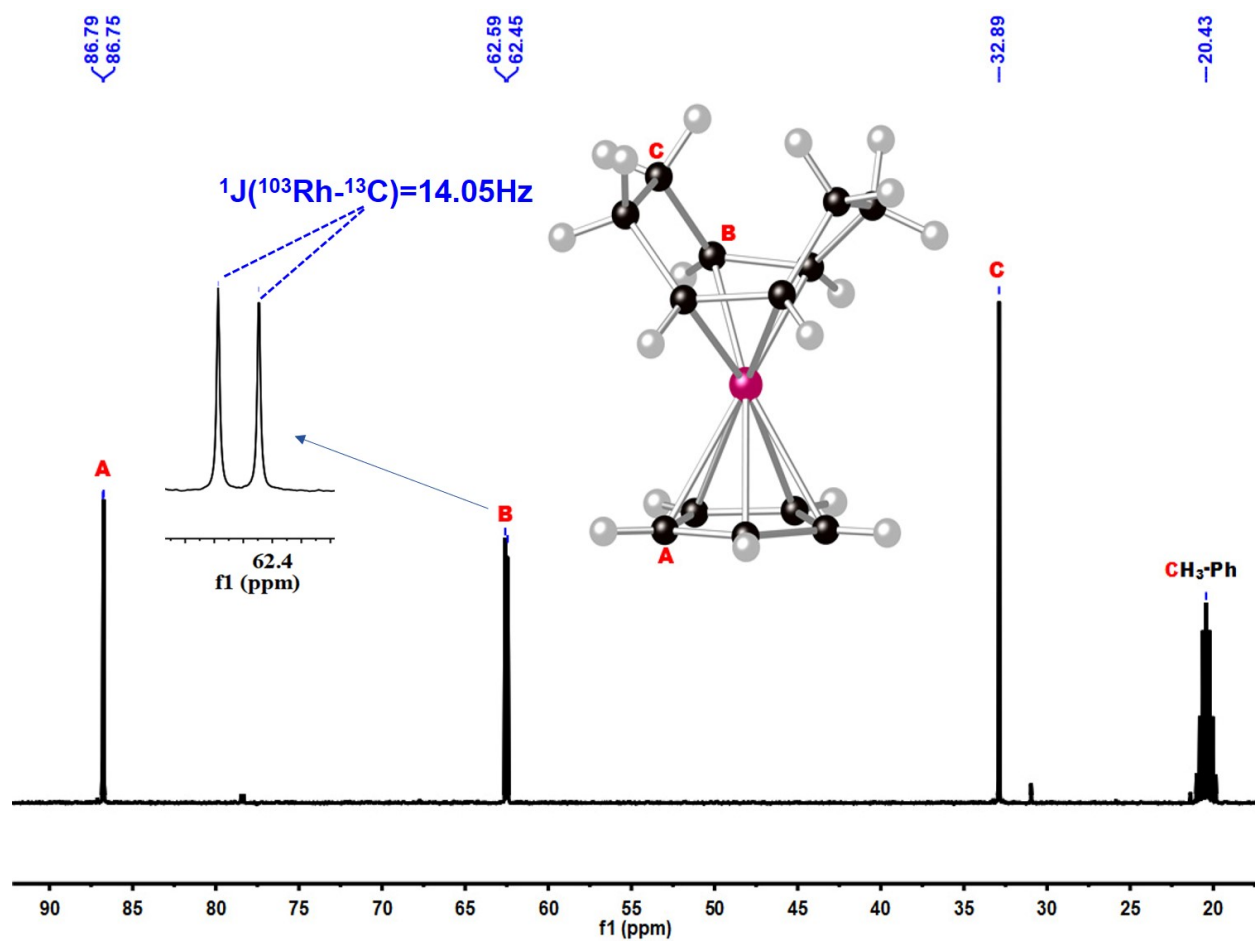


Figure S14 ^{13}C NMR of $\text{CpRh}(\text{COD})$ in D_8 -toluene at room temperature, with all C atoms being labeled.

Table S6 Selected Crystallographic, Data Collection, and Refinement Data for [K(18-crown-6)]₂1•2en•2tol and [K(2,2,2-crypt)]₂•0.5en.^a

Identification code	GDOU01	GDOU02
Empirical formula	C ₃₇ H ₆₄ Bi ₂ KN ₂ O ₆ Rh ₂	C ₆₁ H ₁₁₂ Bi ₃ K ₂ N ₅ O ₁₂ Rh ₃
Formula weight	1295.78	2121.42
Temperature/K	150(2)	150(2)
Crystal system	monoclinic	triclinic
Space group	P2 ₁	P-1
<i>a</i> /Å	13.6378(7)	10.8655(6)
<i>b</i> /Å	17.7192(9)	14.0066(8)
<i>c</i> /Å	17.8331(9)	24.6791(14)
α /°	90	85.315(2)
β /°	92.0637(9)	77.690(2)
γ /°	90	84.060(2)
Volume/Å ³	4306.6(4)	3643.0(4)
<i>Z</i>	4	2
ρ_{cal} cg/cm ³	1.999	1.934
μ /mm ⁻¹	9.040	2.771
<i>F</i> (000)	2492.0	2062.0
Crystal size/mm ³	0.39 × 0.27 × 0.18	0.20 × 0.12 × 0.09
Radiation	MoK α (λ = 0.71073)	synchrotron (λ = 0.41328)
2 θ range for data collection/°	3.696 to 59.996	2.522 to 33.84
Index ranges	-18 ≤ <i>h</i> ≤ 19, -24 ≤ <i>k</i> ≤ 24, -24 ≤ <i>l</i> ≤ 25	15 ≤ <i>h</i> ≤ 15, -19 ≤ <i>k</i> ≤ 19, -34 ≤ <i>l</i> ≤ 34
Reflections collected	43747	131105
Independent reflections	24120 [<i>R</i> _{int} = 0.0329, <i>R</i> _{sigma} = 0.0650]	20698 [<i>R</i> _{int} = 0.0576, <i>R</i> _{sigma} = 0.0406]
Data/restraints/parameters	24120/1130/1110	20698/13/776
Goodness-of-fit on <i>F</i> ²	1.000	1.000
<i>R</i> ₁ / <i>wR</i> ₂ [<i>I</i> ≥ 2 σ (<i>I</i>)]	0.0357, 0.0652	0.0230, 0.0536
<i>R</i> ₁ / <i>wR</i> ₂ [all data]	0.0499, 0.0682	0.0261, 0.0547
Largest diff. peak/hole /eÅ ⁻³	2.13/-1.14	2.50/-2.01
CCDC number	2220838	2220839

^aSee the Crystallographic Studies Section for details on the refinement